
Scalable Learning of Independent Cascade Dynamics from Partial Observations

Mateusz Wilinski
University of Warsaw
wilinski.mateusz@gmail.com

Andrey Y. Lokhov
Theoretical Division
Los Alamos National Laboratory
lokhov@lanl.gov

Abstract

Spreading processes play an increasingly important role in modeling for diffusion networks, information propagation, marketing, and opinion setting. Recent real-world spreading events further highlight the need for prediction, optimization, and control of diffusion dynamics. To tackle these tasks, it is essential to learn the effective spreading model and transmission probabilities across the network of interactions. However, in most cases the transmission rates are unknown and need to be inferred from the spreading data. Additionally, full observation of the dynamics is rarely available. As a result, standard approaches such as maximum likelihood quickly become intractable for large network instances. In this work, we study the popular Independent Cascade model of stochastic diffusion dynamics. We introduce a computationally efficient algorithm, based on a scalable dynamic message-passing approach, which is able to learn parameters of the effective spreading model given only limited information on the activation times of nodes in the network. Importantly, we show that the resulting model approximates the marginal activation probabilities that can be used for prediction of the spread.

1 Introduction

Spreading processes on networks have seen an increasing interest in the domains related to modeling of infectious diseases, regulatory networks, marketing and opinion dynamics. Constructing an effective spreading model from available spreading data is crucial for development of efficient control strategies for an optimal dissemination or mitigation of diffusion [1, 2]. In a realistic setting, the model and parameters, as well as propagation paths are unknown, and one is left at most with several observed diffusion traces. Moreover, even this information is not fully available since the time-stamps of nodes activations are not communicated from each node in the network. This motivates the development of efficient algorithms that can infer the effective spreading models from incomplete information.

In the recent years, the problem of diffusion model recovery from full observations has been relatively well understood through a series of work focusing on heuristic and exact algorithms including the maximum likelihood type approaches [3, 4, 5, 6, 7, 8]. These methods allow one to recover the parameters of the model, as well as the structure of the diffusion graph. Comparably, much less has been done on the side of parameter recovery in the case of partial observations. This is primarily due to the hardness of the estimation in this case, where maximum likelihood marginalized over the hidden observations quickly becomes computationally prohibitive with the number of hidden nodes [9]. The work [10] primarily considered the case of tree graphs, and studied the network reconstruction problem in the setting where only initial and final states of the dynamics are observed. This setting has been further explored in [11] and very recently in [12] for more general graphs. On the other hand, [13] addressed the structure learning problem in the case of missing information in

time through relaxation optimization techniques under the assumption that full probabilistic trace for each vertex is available.

An algorithm for learning model parameters based on the collective information on transmission probabilities contained in the marginals of model computed through a message-passing approach has been suggested in [9]. Although this method provides a low estimation error and is computationally efficient compared to the marginalized likelihood, it still suffers from the computational complexity that scales cubically in the system size for each step of the gradient descent, which limits the applicability of the method to small systems only with an order of dozens of nodes. The main computational bottleneck consists in an efficient evaluation of the gradient of the objective function. In this work, we overcome this limitation by providing an exact method that computes the gradient in a time linear with respect to the dimension of the problem, allowing for an application of the algorithm to realistic networks with millions of nodes. We illustrate the approach on the popular Independent Cascade (IC) model [14, 1] that is often used to model network information diffusion, although it can be generalised to other stochastic dynamic models.

Typically, the main interest for learning the spreading model from data consists in its subsequent use for solving optimization, control, or inference tasks. This setting is sometimes referred to as “learning for inference”, or “inferning” [15]. In the case of diffusion models considered here, the quantity of interest for inference and optimization is given by marginal probabilities of activation, that in particular give access to the expected size of the diffusion spread [16]. Here, we show that with the choice of dynamic message-passing as an inference method, the model learned using the same approach makes the best guess in approximating marginal probability distributions. This result is somewhat similar in spirit to the line of works that address the problem of direct estimation of influence functions from samples [17, 18, 19, 20], with the difference that we are interested in a well-defined model in a given class that can be used for other tasks. Hence, this line of research is complementary to the present contribution where we assume a well-defined model and develop an analytical method for scalable estimation of the explicitly parametrized influence function.

2 Model

We define the diffusion network as $G = (V, E)$, where V is the set of nodes and E is the set of edges. In the IC model, each node can be in either of two states: active or inactive. Node i activated at time t has a single chance to activate its inactive neighbor j at time $t + 1$ with probability α_{ij} associated with the edge $(i, j) \in E$. A single cascade starts with a set of initially active nodes and continues until the dynamics dies out, or at most for a predefined number of steps T . For simplicity, we assume that the transmission probabilities are symmetric, $\alpha_{ij} = \alpha_{ji}$, what follows can be extended to the asymmetric case as well.

Since each node can be activated not more than once, every cascade c can be fully described by a set of activation times $\Sigma^c \equiv \{\tau_i^c\}_{i \in V}$. Additionally, if node i was not activated at all, we by definition assign T as its activation time. The full available information will be denoted as $\Sigma = \bigcup_c \Sigma^c$. In what follows, for simplicity we focus on cascades starting from a single node source. This setting can be straightforwardly generalized to initial conditions with several sources.

In practice, full observation of cascades is rarely available, and hence we split Σ into observed Σ_O and hidden Σ_H parts. The former is the set of observed activation times, whereas the latter consists of unobserved activation times. Our goal is to learn an effective dynamical model from the set of cascades Σ_O . The learned model may provide information on the parameters of the model, i.e. as a result we recover $\Omega \equiv \{\alpha_{ij}\}_{(i,j) \in E}$ that will be on average close to the parameters of the original model used to generate data, denoted by $\Omega^* \equiv \{\alpha_{ij}^*\}_{(i,j) \in E}$. Additionally, the learned model can be used for subsequent prediction, optimization, or inference task. As we show next, even in the case where reconstructed model parameters do not closely match the original parameters of the model, message-passing equations applied to resulting model make a better prediction of the marginals compared to the ground truth parameters.

3 Methods

In the case of full observations, it is possible to explicitly write the likelihood of observed data Σ under the assumption of given set of parameters Ω and IC model dynamics. This likelihood factorises

across cascades and nodes:

$$P(\Sigma|\Omega) = \prod_{c \in C} \prod_{i \in V} P_i(\tau_i^c | \Sigma^c, \Omega), \quad (1)$$

where C is the set of all cascades. Such factorized form of the equation makes it possible to efficiently learn Ω^* via maximum likelihood approach.

Maximum likelihood approach becomes inefficient as we lose full information about activation times. Likelihood calculation would require marginalizing over all potential unknown activation times, while these sums grow exponentially with the number of unobserved nodes, making it intractable for large networks. To deal with this limitation, [9] proposed to approximate the full probability in a mean-field fashion and consider a cost function in a form of a product over marginal probabilities:

$$P(\Sigma_O|\Omega) \approx \prod_{c \in C} \prod_{i \in O} p_i^c(\tau_i^c), \quad (2)$$

where $p_i^c(\tau_i^c)$ are marginal probabilities that depend on the model parameters. These marginals can be efficiently estimated using the Dynamic Message Passing (DMP) equations. Despite successfully recovering parameters in several test cases, the algorithm was only demonstrated for small networks up to 30 nodes. The reason is a limited computational efficiency of the proposed algorithm, where each step of the gradient computation has complexity $O(|E|^2TM)$, where M is the number of different initial conditions in the observed cascades. In this work, we revisit the objective function proposed in [9] and provide an efficient learning algorithm that has a single update step complexity $O(|E|TM)$ with M upper bounded by the size of the graph N , which will allow to apply it to realistic sparse networks with millions of nodes. In what follows, we first revisit the DMP equations for the IC model, and then state our optimization framework.

3.1 Dynamic Message-Passing Equations

In this section, we present DMP equations that approximate $\{p_i^c(t)\}_{i \in V}$ – the set of marginal probabilities that each node $i \in V$ is active at time t under the cascade c with a given initial condition. For tree graphs, estimated marginal probabilities are exact. The computation is performed with additional quantities called messages $p_{j \rightarrow i}^c(t)$, which have a meaning of probabilities of node j being active at time t on an auxiliary graph where i has been removed. These probabilities can be calculated by solving a following system of equations:

$$p_i^c(t) = 1 - (1 - \bar{p}_i^c) \prod_{k \in \partial i} \left(1 - \alpha_{ki} \cdot p_{k \rightarrow i}^c(t-1)\right), \quad (3)$$

$$p_{j \rightarrow i}^c(t) = 1 - (1 - \bar{p}_j^c) \prod_{k \in \partial j \setminus i} \left(1 - \alpha_{kj} \cdot p_{k \rightarrow j}^c(t-1)\right), \quad (4)$$

where $\bar{p}_i^c = p_i^c(0)$. Properties of these equations have been extensively studied in [16], and are related to the DMP equations for the popular SIR model in the limit of deterministic recovery [21, 22], while the large-time form of these equations have been previously derived in [23, 24]. Although exactness of DMP predictions are guaranteed on tree graphs only, they often provide accurate approximations on sparse but loopy graphs. Moreover, for general graphs, the solution of above equations provides an upper bound for marginal probabilities [16]. Note that for given set of parameters, the solution depends only on the initial state \bar{p}_i^c . Next section explains how DMP equations combined with a Lagrangian formulation of the learning problem can be used to estimate model parameters $\{\alpha_{ij}\}_{(i,j) \in E}$.

3.2 Constrained Optimization Based Learning Framework

The model estimation problem can be expressed as a constrained optimization problem, where the objective function is inspired by (2) and the constraints express the fact that the marginals are estimated using DMP equations (3)-(4). In [9], the gradient of the objective has been estimated via a direct derivative of the DMP equations. Instead, here we use a standard Lagrangian formulation for the constrained optimization problem:

$$\mathcal{L} = \underbrace{\mathcal{O}}_{\text{objective}} + \underbrace{\mathcal{C}}_{\text{constraints}}. \quad (5)$$

We choose the objective function as the logarithm of the approximation (2):

$$\begin{aligned}\mathcal{O} &= \log P(\Sigma_O|\Omega) \\ &\approx \sum_{c \in \mathcal{C}} \sum_{i \in \mathcal{O}} \log \left(p_i^c(\tau_i^c) \cdot \mathbb{1}_{(\tau_i^c < T)} - p_i^c(\tau_i^c - 1) \cdot \mathbb{1}_{(\tau_i^c > 0)} + \mathbb{1}_{(\tau_i^c = T)} \right).\end{aligned}\quad (6)$$

Assuming that each cascade starts in a single node, all cascades can be divided into classes according to their initial conditions. Let us denote the set of such classes as S . Notice that for given parameters, the number of different sets of messages and marginals is of the same size as S , because they only differ by initial conditions. As a result we can rewrite the objective as follows:

$$\begin{aligned}\mathcal{O} &= \log P(\Sigma_O|\Omega) \\ &\approx \sum_{s \in S} \sum_{i \in \mathcal{O}} \sum_{\tau_i^s} m^{\tau_i^s} \log \left(p_i^s(\tau_i^s) \cdot \mathbb{1}_{(\tau_i^s < T)} - p_i^s(\tau_i^s - 1) \cdot \mathbb{1}_{(\tau_i^s > 0)} + \mathbb{1}_{(\tau_i^s = T)} \right),\end{aligned}\quad (7)$$

where $m^{\tau_i^s}$ is the number of cascades in class s for which node i was activated at time τ_i^s .

The constraints are given by DMP equations (3)-(4) re-weighted by Lagrange multipliers:

$$\begin{aligned}\mathcal{C} &= \sum_{s \in S} \sum_{t=0}^{T-1} \sum_{i \in V} \lambda_i^s(t+1) \left(p_i^s(t+1) - 1 + (1 - \bar{p}_i^s) \prod_{k \in \partial i} \left(1 - \alpha_{ki} \cdot p_{k \rightarrow i}^s(t) \right) \right) \\ &+ \sum_{s \in S} \sum_{t=0}^{T-1} \sum_{(i,j) \in E} \lambda_{i \rightarrow j}^s(t+1) \left(p_{i \rightarrow j}^s(t+1) - 1 + (1 - \bar{p}_i^s) \prod_{k \in \partial i \setminus j} \left(1 - \alpha_{ki} \cdot p_{k \rightarrow i}^s(t) \right) \right),\end{aligned}\quad (8)$$

where $\lambda_i^s(t)$ and $\lambda_{i \rightarrow j}^s(t)$ are Lagrange multipliers corresponding respectively to equations (3) and (4).

The resulting expressions for all the quantities can be found by differentiating the Lagrangian. Differentiation over marginals yields expressions for $\lambda_i^s(t)$ multipliers for all sources s and times t :

$$\begin{aligned}\frac{\partial \mathcal{L}}{\partial p_i^s(t)} &= \lambda_i^s(t) + \frac{m^{\tau_i^s} \cdot \mathbb{1}_{(t=\tau_i^s)} \cdot \mathbb{1}_{(\tau_i^s < T)}}{p_i^s(\tau_i^s) - p_i^s(\tau_i^s - 1) \cdot \mathbb{1}_{(\tau_i^s > 0)}} \\ &+ \frac{m^{\tau_i^s} \cdot \mathbb{1}_{(t=\tau_i^s-1)} \cdot \mathbb{1}_{(\tau_i^s > 0)}}{p_i^s(\tau_i^s - 1) - p_i^s(\tau_i^s) \cdot \mathbb{1}_{(\tau_i^s < T)} - \mathbb{1}_{(\tau_i^s = T)}}.\end{aligned}\quad (9)$$

One direct consequence of this is that $\lambda_i^s(t) = 0 \forall t \notin \{\tau_i^s, \tau_i^s - 1\}$. The $\lambda_{i \rightarrow j}^s(t)$ multipliers can be obtained from the derivatives over messages. For $t < T$ we get

$$\begin{aligned}\frac{\partial \mathcal{L}}{\partial p_{i \rightarrow j}^s(t)} &= \lambda_{i \rightarrow j}^s(t) - \lambda_j^s(t+1) \alpha_{ij} (1 - \bar{p}_j^s) \prod_{m \in \partial j \setminus i} \left(1 - \alpha_{mj} \cdot p_{m \rightarrow j}^s(t) \right) \\ &- \sum_{k \in \partial j \setminus i} \lambda_{j \rightarrow k}^s(t+1) \alpha_{ij} (1 - \bar{p}_j^s) \prod_{m \in \partial j \setminus \{i, k\}} \left(1 - \alpha_{mj} \cdot p_{m \rightarrow j}^s(t) \right).\end{aligned}\quad (10)$$

For $t = T$, the expression simplifies to

$$\frac{\partial \mathcal{L}}{\partial p_{i \rightarrow j}^s(T)} = \lambda_{i \rightarrow j}^s(T),\quad (11)$$

which allows to calculate all $\lambda_{i \rightarrow j}^s(t)$ in an inductive manner, starting from T and using $\lambda_{i \rightarrow j}^s(t+1)$ to compute multipliers for $t < T$. Finally, derivatives over parameters α_{ij} read

$$\begin{aligned}
\frac{\partial \mathcal{L}}{\partial \alpha_{ij}} = & - \sum_{s \in S} \sum_{t=0}^{T-1} \lambda_i^s(t+1) p_{j \rightarrow i}^s(t) (1 - \bar{p}_i^s) \prod_{m \in \partial i \setminus j} \left(1 - \alpha_{mi} \cdot p_{m \rightarrow i}^s(t)\right) \\
& - \sum_{s \in S} \sum_{t=0}^{T-1} \lambda_j^s(t+1) p_{i \rightarrow j}^s(t) (1 - \bar{p}_j^s) \prod_{m \in \partial j \setminus i} \left(1 - \alpha_{mj} \cdot p_{m \rightarrow j}^s(t)\right) \\
& - \sum_{s \in S} \sum_{t=0}^{T-1} \sum_{k \in \partial i \setminus j} \lambda_{i \rightarrow k}^s(t+1) p_{j \rightarrow i}^s(t) (1 - \bar{p}_i^s) \prod_{m \in \partial i \setminus \{j, k\}} \left(1 - \alpha_{mi} \cdot p_{m \rightarrow i}^s(t)\right) \\
& - \sum_{s \in S} \sum_{t=0}^{T-1} \sum_{k \in \partial j \setminus i} \lambda_{j \rightarrow k}^s(t+1) p_{i \rightarrow j}^s(t) (1 - \bar{p}_j^s) \prod_{m \in \partial j \setminus \{i, k\}} \left(1 - \alpha_{mj} \cdot p_{m \rightarrow j}^s(t)\right).
\end{aligned} \tag{12}$$

Notice that for non-zero parameters α_{ij} , the expressions above can be significantly simplified:

$$\frac{\partial \mathcal{L}}{\partial \alpha_{ij}} = - \frac{1}{\alpha_{ij}} \sum_{s \in S} \sum_{t=0}^{T-1} (\lambda_{i \rightarrow j}^s(t) p_{i \rightarrow j}^s(t) + \lambda_{j \rightarrow i}^s(t) p_{j \rightarrow i}^s(t)). \tag{13}$$

Now, we can use gradient components (12) to update parameters α_{ij} :

$$\alpha_{ij} = \alpha_{ij} + \varepsilon \cdot \frac{\partial \mathcal{L}}{\partial \alpha_{ij}}, \tag{14}$$

where ε is a learning rate. The resulting algorithm can be expressed in a form of forward-backward iterations:

1. Start with initial parameter guess α_{ij} ;
2. Calculate marginals and messages using forward DMP equations (3)-(4);
3. Use estimated marginals and messages to compute Lagrange multipliers through the backward equations (11) and (10);
4. Use equations (12) and (14) to update parameters α_{ij} ;
5. Go back to step 2, and repeat the process with updated α_{ij} , until the global convergence of the algorithm.

Calculating marginals using DMP requires complexity $O(|E|T)$ and needs to be done for each different initial point of all available cascades, resulting in the worst-case computational complexity $O(|E|TM)$. In the case of single-node initial conditions, this complexity is upper-bounded by $O(|E|TN)$. Lagrange multipliers require the same computational complexity, since backward equations are equivalent to dynamic message-passing equations in the dual space. Finally, derivatives with respect to $\{\alpha_{ij}\}_{(i,j) \in E}$, as seen from equation (12), are computed with the same computational complexity. As a result, a single update step in our learning algorithm has a complexity $\min [O(|E|TM), O(|E|TN)]$. In the next section, we test the proposed algorithm on synthetic data.

4 Results

The accuracy of DMP equations are only guaranteed on tree graphs, and hence it is interesting to empirically evaluate the performance of our algorithm on a variety of topologies, including random regular graphs and regular lattices with a very large number of loops. Naturally, our main focus will be the case of partial observations, where maximum likelihood based approaches are not applicable. In the setting of learning for inference, we show that even in the case of loopy non tree-like networks, our algorithm approximates the marginals well due to the recovery of the best *effective* parameters α_{ij} that try to match the outcome of the DMP equations with marginals, and do so better compared to the ground-truth values α_{ij}^* .

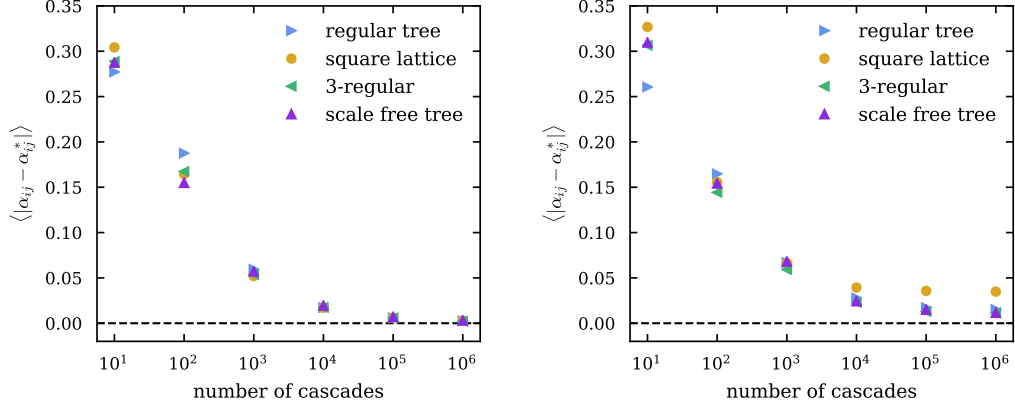


Figure 1: Average difference between inferred α_{ij} and real α_{ij}^* parameters in ℓ_1 norm, as a function of number of available cascades in the case of full observations of cascades. Each point is averaged over five different networks and five different sets of parameters α_{ij}^* (sampled from a uniform distribution between zero and one). All networks contain $N = 100$ nodes. *Left*: Observation time $T = 5$. *Right*: Observation time $T = 10$.

4.1 Estimation of Model Parameters from Partial Observations

In our tests throughout this section, parameters α_{ij}^* that are used for generating data are sampled uniformly from $[0, 1]$. Each cascade is generated independently from the IC model with finite observation time T , varying from 5 to 20. All points in the plots are averaged over multiple realisations of parameters α_{ij}^* and network structures. In all presented results, we choose $\alpha_{ij} = 0.5 \forall (ij) \in E$ as initialization of the learning procedure.

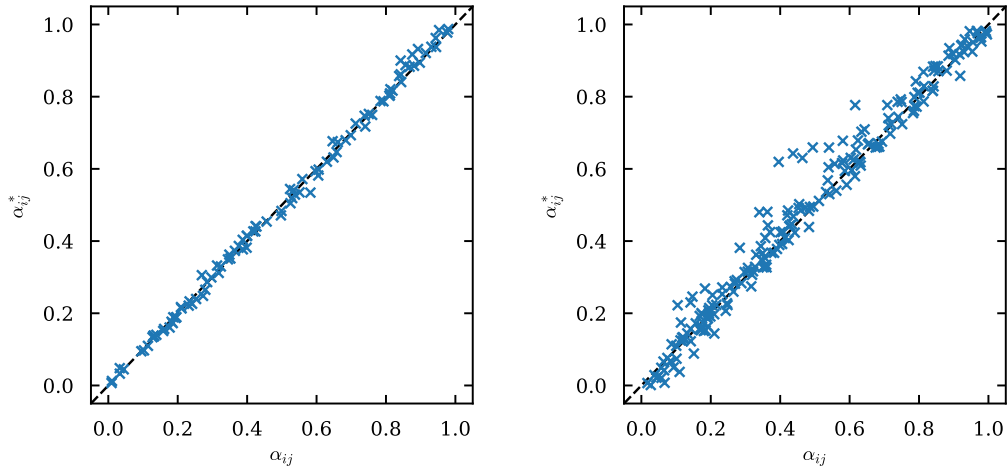


Figure 2: Scatter plot between original model parameters α_{ij}^* and estimated ones α_{ij} . Single instance with $N = 100$ nodes and $M = 5 \cdot 10^4$ cascades of length $T = 10$ is presented. *Left*: Regular tree of degree three. *Right*: Square lattice.

In order to get a flavor of typical reconstruction errors as a function of network topology, we calibrate our approach on the case of full observations. The results for this simplest setting, for different network types, are shown in Fig. 1. In particular, we test error decay on a regular tree of degree three, a scale-free tree, a random regular graph of degree three, and a square lattice. The apparent difference between left and right subplots of Fig. 1 is a result of loops affecting the accuracy of

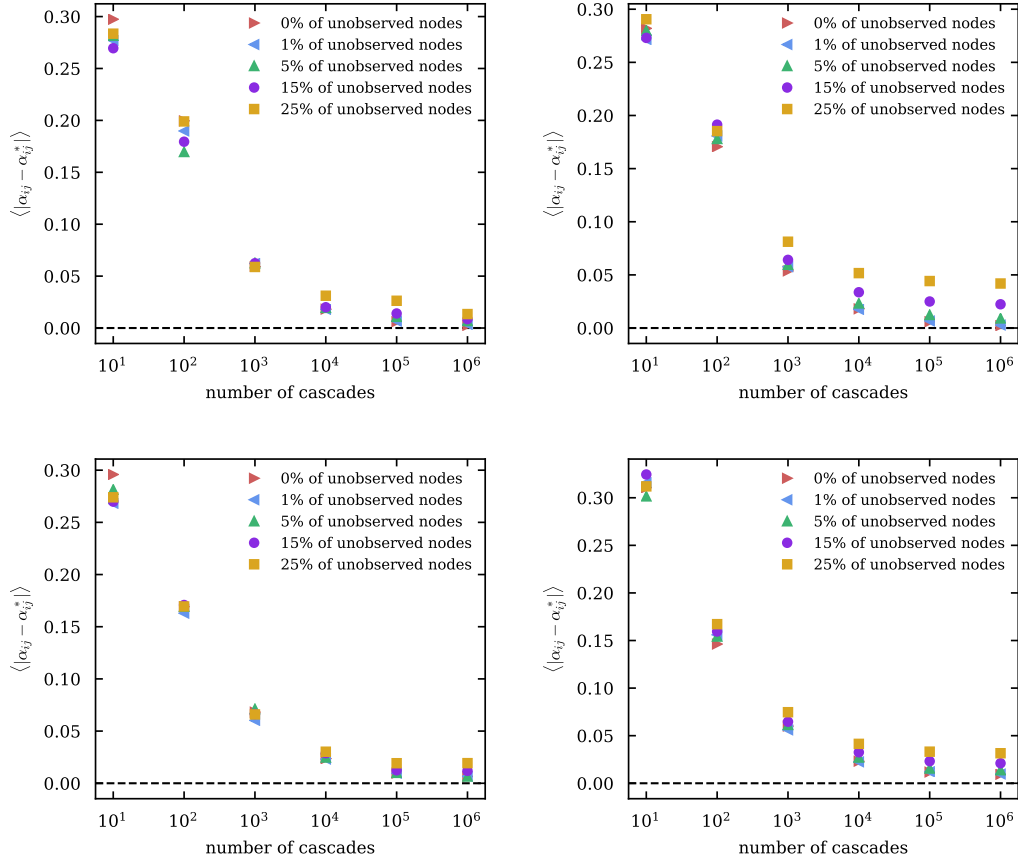


Figure 3: Average difference between inferred α_{ij} and real α_{ij}^* parameters in ℓ_1 norm, as a function of number of available cascades in the case of partial observations of cascades. Each point is averaged over five different networks and five different sets of parameters α_{ij}^* (sampled from a uniform distribution between zero and one). All networks contain $N = 100$ nodes. Unobserved nodes were picked at random. For tree graphs, edges adjacent to unobserved leaves were excluded. *Left:* Regular trees of degree three. *Right:* Random three-regular graphs. *Upper:* Observation time $T = 5$. *Lower:* Observation time $T = 10$.

DMP equations: When the observation time horizon is short, even though the graph is loopy, the spreading is effectively happens on a tree-like region where DMP equations are exact. As T increases, information spreads through loops that start to have an effect for the accuracy of predictions of marginals, and hence on the recovered parameters. For the adversarial case of regular grid, the error saturates to a finite value for $T = 10$ even for a large number of samples. This is expected due to the presence of systematic short loops.

To give a better intuition about the nature of the growing distance between estimated and true parameters, we present a comparison between the two for a single estimation in Fig. 2. As expected, estimation error on the right panel (square lattice) is higher than for a regular tree (left panel), and all recovered parameters oscillate around correct values.

Let us now move to a more interesting case of reconstructing parameters when only part of the information is available. To test the accuracy of our method, we randomly pick a fraction of nodes and hide their activation times throughout all cascades. Results for this more challenging setting are shown in Fig. 3. We test two types of networks, regular trees and regular random graphs, both for shorter, $T = 5$, and longer, $T = 10$, cascades. In the case of trees, we neglected edges that connect unobserved leaves with the rest of the network, since estimation of their spreading parameters is impossible with any algorithm. These results show that α_{ij}^* can be efficiently estimated, even with

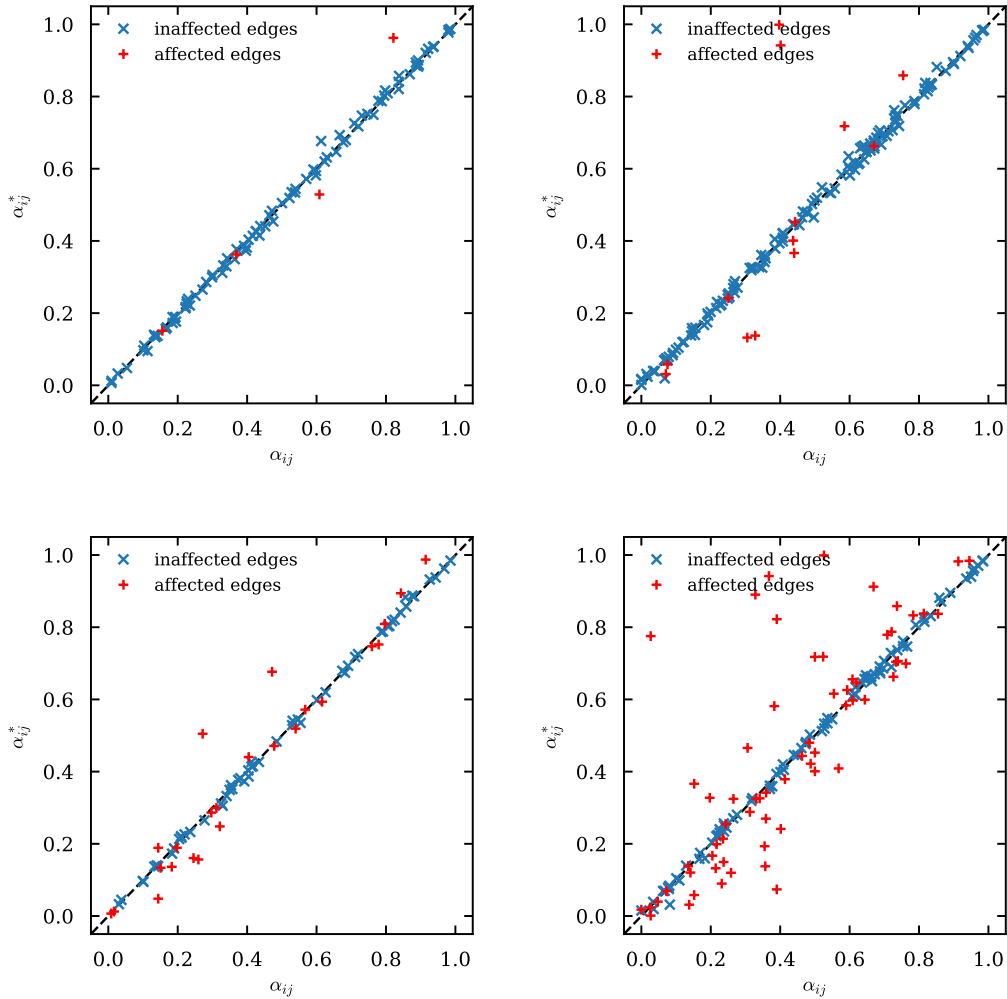


Figure 4: Scatter plot between original model parameters α_{ij}^* and estimated ones α_{ij} . Single instance with $N = 100$ nodes and $M = 5 \cdot 10^4$ cascades of length $T = 5$ is presented. Unobserved nodes were picked at random. For tree graphs, edges adjacent to unobserved leaves were excluded. *Left:* Regular trees of degree three. *Right:* Random three-regular graphs. *Upper:* Percentage of unobserved nodes $d = 5\%$. *Lower:* Percentage of unobserved nodes $d = 25\%$.

25% of unobserved nodes, as long as we have enough data. Moreover, the reconstruction results get better with the growing observation time for these tree-like cases. Single instance reconstruction results of the estimation procedure are shown in Fig. 4, proving that the algorithm is still able to efficiently recover the parameters of affected edges, i.e. the ones connected to unobserved nodes.

4.2 Prediction of Marginal Probabilities

As explained in the introduction, in many applications falling under the “learning for inference” setting [15], we are less interested in an accurate recovery of the underlying model parameters, but instead want to create an *effective* model that succeeds in correctly predicting the marginal distributions that can subsequently be used for control, optimization, or learning tasks. Here, we demonstrate that our approach naturally recovers the best effective parameters that lead to a better approximation of the marginals in the case where DMP is used as an inference complexity due to its attractive computational complexity comparable to a single run of the Monte-Carlo simulation [16].

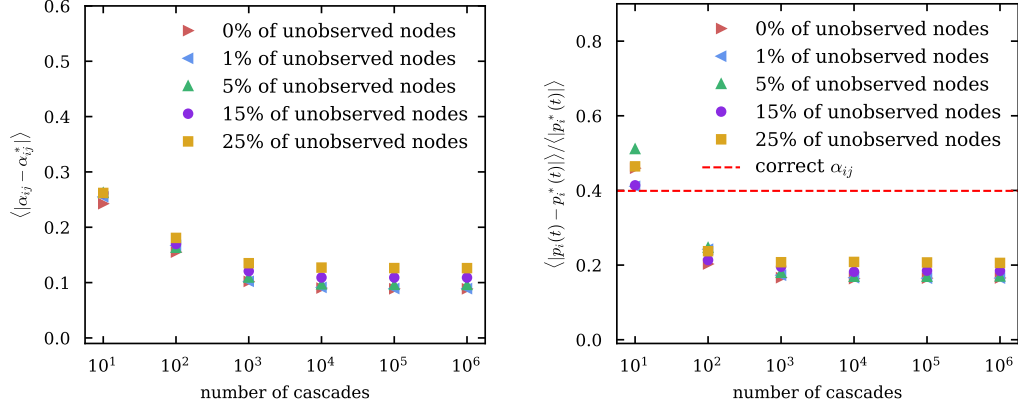


Figure 5: Illustration of the effective model concept, where our algorithm recovers the set of parameters that try to match marginal probabilities observed in the data. Both panels correspond to a challenging square lattice topology with $N = 100$ nodes and cascades of length $T = 20$. *Left*: Distance between true α_{ij}^* and estimated α_{ij} parameters. *Right*: Relative distance between real (computed through Monte-Carlo) and estimated (estimated via DMP) marginals. The red line represents the relative distance between real marginals and the ones obtained by using the ground-truth parameters α_{ij} within the DMP equations.

As already mentioned, the primary source of error in DMP equations are related to loops: Their presence may result in overestimating parameters to account for DMP neglecting information on some spreading paths. To study this effect in more details, we focused on the most challenging case of a square lattice with many short loops, in an adversarial case of very long cascades with $T = 20$. As shown in left panel of Fig. 5, this represents a challenging setting in terms of prediction of marginals using the DMP-based algorithm, which results in a finite error for parameter estimation even for a large number of cascades. It is however important to note that the algorithm is not optimized to parameter recovery, but instead attempts to maximize the probability of observed marginal probabilities, as seen from the objective function (2). Hence, the recovered effective parameters should be the ones that attempt to match the marginal probabilities observed in the data. Right panel from Fig. 5 shows relative distance between true and estimated marginals, and demonstrates that DMP equations run with reconstructed parameters produce a better approximation of real marginal probabilities, compared to DMP predictions using the ground-truth parameters α_{ij}^* . Importantly, this observation holds in the partial information regime. This observation yields a promising avenue for building *effective* models, which may not reflect the real spreading parameters, but allow for a more accurate prediction of the dynamics, and hence can be used for tasks such as influence maximization [1] or control [2].

These results further confirm the need for consistency in the “learning for inference” approach. Inference tasks are typically computationally harder compared to their learning counterpart. An ideal estimation procedure would perfectly reconstruct model parameters, that may yield inaccurate predictions of the dynamic outcome due to intrinsic errors in approximate inference algorithms. Our analysis shows that a consistent use of an approximate scheme in both learning and inference task leads to an effective model that has a much stronger prediction power. This concept further motivates the extension of the search for effective models outside of the original class (for instance, allowing for a different network topology), as long as the goal consists in an accurate prediction of the dynamics.

5 Conclusions

Incomplete information about the dynamics significantly complicates the maximum likelihood approach: From a simple combination of local independent convex optimisations, it becomes to a computationally expensive task, with complexity growing exponentially with the number of unobserved nodes. In this paper, we propose a novel approximate learning algorithm based on a dynamic message-passing approach. The method achieves a significantly better scalability compared

to existing approximate methods such as [9]. Moreover, even in a loopy regime which is adversarial for message-passing techniques, our method explores the space of parameters in search of an effective model that achieves a better prediction of the dynamics. We anticipate that scalability and prediction qualities of our algorithm will be useful for real-world applications where large amounts of incomplete data is available and a need of reliable scenario testing is essential. Although our study used the standard discrete-time IC model for illustration, DMP can be generalised to more complex dynamical models [22]. This includes different spreading models, time varying parameters $\alpha_{ij}(t)$, adaptive spreading settings, continuous time dynamics, or temporal networks. Finally, we believe that our approach will be helpful in the task of optimal resource allocation for both monitoring and containment of spreading processes.

Acknowledgments

AYL acknowledges support from the Laboratory Directed Research and Development program of Los Alamos National Laboratory under project number 20200121ER.

Appendix

A1 Choice of the learning rate

All of the numerical results presented in the paper were obtained with the learning rate $\varepsilon = c \frac{N}{MT}$ in equation (14), where N is the number of nodes, M is the number of cascades, T is the length of cascades, and c is a small constant (the same for all networks) ensuring that the step is not too large. This normalisation of the gradient step is convenient because it results in very similar number of steps until global convergence across different network sizes for similar level of available information. This effect is demonstrated in Fig. A1 in the case of random three regular graph with varying size and accordingly rescaled number of cascades. As a consequence of this observation, it is easy to estimate the running time of the algorithm based on the running time of a single iteration. In the next section, we show the empirical scalability per iteration step of the proposed algorithm as a function of problem parameters.

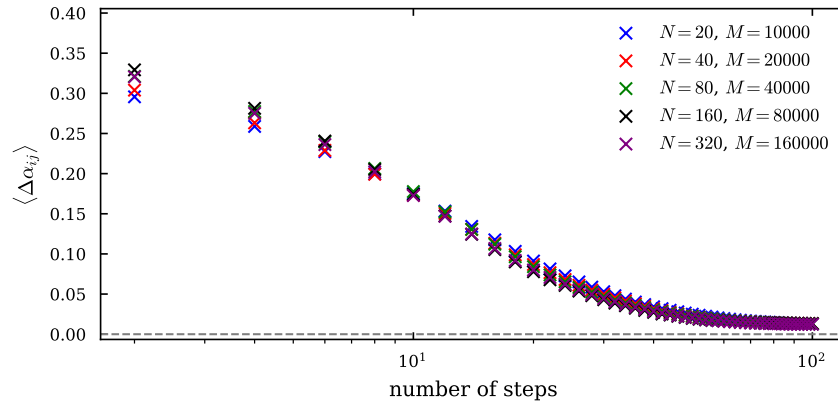


Figure A1: Convergence of the algorithm as a function of number of gradient descent steps, measured by the change of α_{ij} after each consecutive step. The simulations were done with cascades of length $T = 10$. All the points were obtained using the learning rate $\varepsilon = c \frac{N}{MT}$ in the equation (14).

A2 Empirical algorithmic complexity

As discussed in the main text, the overall computational complexity of our learning algorithm is $\mathcal{O}(|E|TM)$ for $M < N$, and $\mathcal{O}(|E|TN)$ for $M \geq N$. In this section, we check the empirical scalability of the algorithm. Fig. A2 shows the linearly growing computational time required to

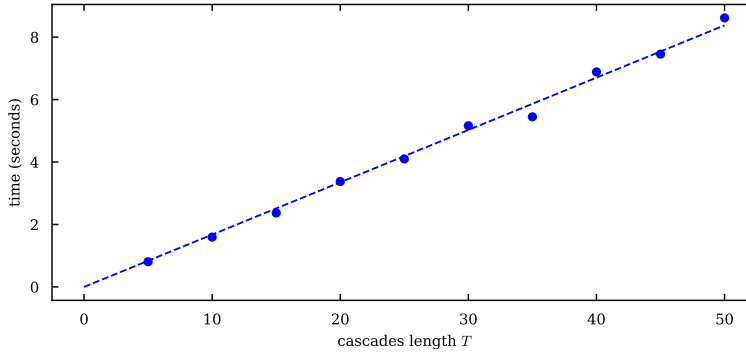


Figure A2: Averaged computational times for a single step of optimisation, as a function of cascade length T . Simulations were made using $M = 100$ cascades on a random three regular graph with $N = 100$ nodes. Each point represents an average over five different realisations of the network. The reference dashed line is the best linear fit with a zero intercept.

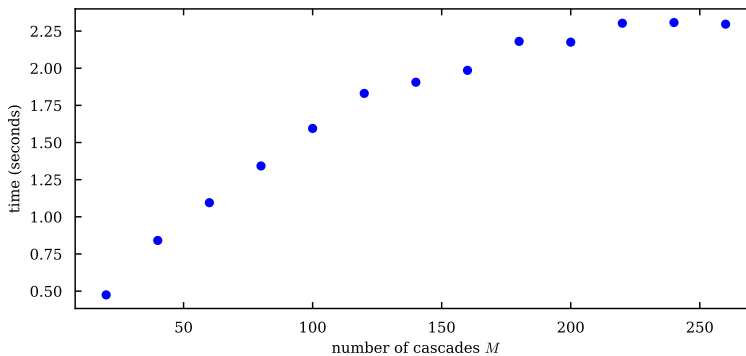


Figure A3: Averaged computational times for a single step of optimisation, as a function of the number of available cascades M . Simulations were made using cascades of $T = 10$ length on a random three regular graph with $N = 100$ nodes. Each point represents an average over five different realisations of the network.

perform one step of the optimisation process as a function of the cascade length T . A more interesting dependence on the number of cascades is shown in Fig. A3. Linear until the number of cascades reaches the order of the network size, the optimization time starts to plateau for larger M once the number of classes saturates to N , which is consistent with the complexity analysis above. Finally, the linear scaling for different network sizes is presented in Fig. A4.

A3 Code and implementation efficiency

The code used to obtain all the results in the paper is available at: <https://github.com/mateuszwilinski/dynamic-message-passing/>. We used a straightforward implementation of the proposed algorithm, where the DMP equations are run for all nodes and edges in the graph. This implementation choice was made so that it is applicable to general initial conditions that include arbitrary initial probability distributions factorized over nodes of the graph [16]. However, for the single-source cascades considered in this paper for simplicity, it is clear that on very large networks one could take advantage of the finite T and restrict the dynamics both in the primal and in the dual space to the part of the network that is reachable by the dynamics. Due to the linear size scalings with the system size, we have checked that our learning scheme can indeed be run on networks with the size on the order of million of nodes. However, at these sizes it would also be beneficial to use better memory managing schemes that load parts of the information dynamically, to avoid the RAM

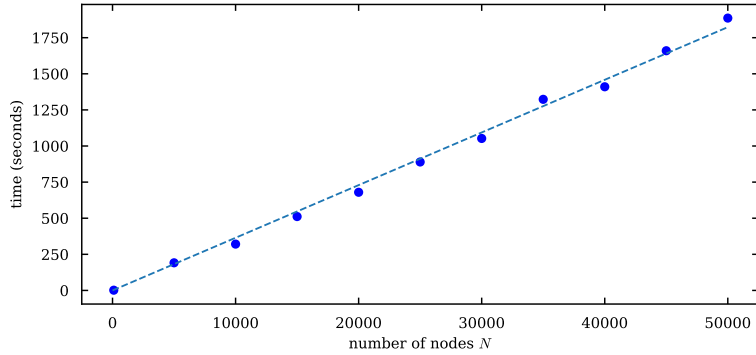


Figure A4: Averaged computational time for a single step of optimisation, as a function of the network size N . Simulations were made using $M = 100$ cascades of $T = 10$ length on a random three regular graphs of different sizes. Each point represents an average over five different realisations of the network. The reference dashed line is the best linear fit with a zero intercept.

saturation on regular machines. Finally, notice that calculations for different can be parallelized, where additionally an asynchronous stochastic version of the gradient descent can be used.

References

- [1] David Kempe, Jon Kleinberg, and Éva Tardos. Maximizing the spread of influence through a social network. In *Proceedings of the ninth ACM SIGKDD international conference on Knowledge discovery and data mining*, pages 137–146, 2003.
- [2] Cameron Nowzari, Victor M Preciado, and George J Pappas. Analysis and control of epidemics: A survey of spreading processes on complex networks. *IEEE Control Systems Magazine*, 36(1):26–46, 2016.
- [3] Praneeth Netrapalli and Sujay Sanghavi. Learning the graph of epidemic cascades. *ACM SIGMETRICS Performance Evaluation Review*, 40(1):211–222, 2012.
- [4] Manuel Gomez-Rodriguez, Jure Leskovec, and Andreas Krause. Inferring networks of diffusion and influence. *ACM Transactions on Knowledge Discovery from Data (TKDD)*, 5(4):1–37, 2012.
- [5] Vincent Gripon and Michael Rabbat. Reconstructing a graph from path traces. In *2013 IEEE International Symposium on Information Theory*, pages 2488–2492. IEEE, 2013.
- [6] Bruno Abrahao, Flavio Chierichetti, Robert Kleinberg, and Alessandro Panconesi. Trace complexity of network inference. In *Proceedings of the 19th ACM SIGKDD international conference on Knowledge discovery and data mining*, pages 491–499, 2013.
- [7] Jean Pouget-Abadie and Thibaut Horel. Inferring graphs from cascades: A sparse recovery framework. In *Proceedings of the 32nd International Conference on International Conference on Machine Learning - Volume 37, ICML’15*, page 977–986. JMLR.org, 2015.
- [8] Alfredo Braunstein, Alessandro Ingrosso, and Anna Paola Muntoni. Network reconstruction from infection cascades. *Journal of the Royal Society Interface*, 16(151):20180844, 2019.
- [9] Andrey Likhov. Reconstructing parameters of spreading models from partial observations. In *Advances in Neural Information Processing Systems*, pages 3467–3475, 2016.
- [10] Kareem Amin, Hoda Heidari, and Michael Kearns. Learning from contagion (without time-stamps). In *International Conference on Machine Learning*, pages 1845–1853, 2014.
- [11] Adisak Supeesun and Jittat Fakcharoenphol. Learning network structures from contagion. *Information Processing Letters*, 121:11–16, 2017.
- [12] Keqi Han, Yuan Tian, Yunjia Zhang, Ling Han, Hao Huang, and Yunjun Gao. Statistical estimation of diffusion network topologies. In *2020 IEEE 36th International Conference on Data Engineering (ICDE)*, pages 625–636. IEEE, 2020.

- [13] Emre Sefer and Carl Kingsford. Convex risk minimization to infer networks from probabilistic diffusion data at multiple scales. In *2015 IEEE 31st International Conference on Data Engineering*, pages 663–674. IEEE, 2015.
- [14] Jacob Goldenberg, Barak Libai, and Eitan Muller. Talk of the network: A complex systems look at the underlying process of word-of-mouth. *Marketing letters*, 12(3):211–223, 2001.
- [15] Guy Bresler, Mina Karzand, et al. Learning a tree-structured ising model in order to make predictions. *Annals of Statistics*, 48(2):713–737, 2020.
- [16] Andrey Y Lokhov and David Saad. Scalable influence estimation without sampling. *arXiv preprint arXiv:1912.12749*, 2019.
- [17] Nan Du, Yingyu Liang, Maria Balcan, and Le Song. Influence function learning in information diffusion networks. In *International Conference on Machine Learning*, pages 2016–2024, 2014.
- [18] Harikrishna Narasimhan, David C Parkes, and Yaron Singer. Learnability of influence in networks. In C. Cortes, N. D. Lawrence, D. D. Lee, M. Sugiyama, and R. Garnett, editors, *Advances in Neural Information Processing Systems 28*, pages 3186–3194. Curran Associates, Inc., 2015.
- [19] Xinran He, Ke Xu, David Kempe, and Yan Liu. Learning influence functions from incomplete observations. In *Advances in Neural Information Processing Systems*, pages 2073–2081, 2016.
- [20] Maggie Makar, John Guttag, and Jenna Wiens. Learning the probability of activation in the presence of latent spreaders. In *Thirty-Second AAAI Conference on Artificial Intelligence*, 2018.
- [21] Brian Karrer and Mark EJ Newman. Message passing approach for general epidemic models. *Physical Review E*, 82(1):016101, 2010.
- [22] Andrey Y Lokhov, Marc Mézard, and Lenka Zdeborová. Dynamic message-passing equations for models with unidirectional dynamics. *Physical Review E*, 91(1):012811, 2015.
- [23] Emmanuel Abbe, Sanjeev Kulkarni, and Eun Jee Lee. Nonbacktracking bounds on the influence in independent cascade models. In *Advances in Neural Information Processing Systems*, pages 1407–1416, 2017.
- [24] Rebekka Burkholz and John Quackenbush. Cascade size distributions and why they matter. *arXiv preprint arXiv:1909.05416*, 2019.